Accuracy of Deconvolution Algorithms Assessed by Simulation Studies: Concise Communication

Alvin Kuruc, S. Treves and J. Anthony Parker

Harvard Medical School, Children's Hospital Medical Center, and Beth Israel Hospital, Boston, Massachusetts

Deconvolution has been used to correct first-pass radionuclide angiocardiography for the time course of the delivery of radiopharmaceutical into the cardiopulmonary system. The extreme sensitivity of deconvolution to random errors in the data may account for some of the problems encountered in practice. We implemented several deconvolution algorithms that were suitable for use with the unimodal and multimodal superior vena caval and pulmonary curves found in left-to-right shunt quantification. The sensitivity of the algorithms to random errors was assessed using mathematical test problems degraded with pseudorandom noise. An algorithm that constrained the deconvolved pulmonary curve to be expressable as the non-negative sum of a set of lagged normal curves was found to have the smallest maximum error on the curves tested. Comparison with results from a previously published test problem indicated an error reduction of greater than 50% over previously used algorithms. Use of this algorithm may permit more accurate deconvolution of pulmonary time-activity curves and thereby improve shunt quantification.

J Nucl Med 24: 258–263, 1983

High temporal resolution is essential for optimal visual and numerical analysis of radionuclide angiocardiography. Reasonably good temporal resolution is attained when the radiotracer is injected rapidly as a single compact bolus. Fragmented and/or prolonged injections lead to inadequate angiocardiograms from which it may be difficult or impossible to obtain the desired information. An area where the quality of tracer delivery into the cardiopulmonary system is critical for accurate results is the quantification of left-to-right shunting (*1*,*2*). It may be possible to correct some of these studies for suboptimal delivery of tracer using deconvolution (*3*,*4*). In this procedure, the cardiovascular circulation is modeled as a linear, time-invariant system (*5*). Time-activity curves obtained from regions of interest over the superior vena cava and lungs are taken as the input and output of the system respectively. The unit impulse response (UIR) of the system represents the pulmonary curve that would be obtained from a perfect spike injection at the level of the superior vena cava. Deconvolution has been shown to improve the accuracy of left-to-right shunt quantification in studies performed with prolonged, but not fragmented, delivery of tracer (*3*,*4*).

Deconvolution by exact solution of the convolution equation is an unstable process in the sense that small errors in the data lead to large errors in the computed UIR (*6–9*). This instability may be illustrated by an example. Consider the input function that would be produced by starting a constant infusion of tracer at the level of the superior vena cava. The corresponding output function would be equal to the integral of the UIR of the system. In this special case, deconvolution is equivalent to point-by-point differentiation of the recorded output function. Clearly small data errors in the output function will lead to large errors in the point-by-point estimates

Received Mar. 31, 1982; revision accepted Nov. 19, 1982.

For reprints contact: S. Treves, MD, Div. of Nucl. Med., Children's Hospital Medical Center, 300 Longwood Ave., Boston, MA 02115.

of the derivatives. In the general case, UIR estimates computed by exact deconvolution often contain negative values and high-frequency oscillations that are physiologically unrealistic.

In practice, the UIR may be estimated with a well-behaved approximate solution to the convolution equation that is judged to be physically plausible. The accuracy of such an estimate is open to question, since in most cases the true UIR is not obtainable. Reconvolution of the estimated UIR with the input should produce a function that is approximately equal to the output. In other words, the UIR estimate should have a small reconvolution error. However, this is not a sufficient test to ensure the accuracy of the UIR estimate, since functions that are physically implausible will often have a small reconvolution error (*6*). It is thus necessary to verify the stability of deconvolution algorithms with regard to random data errors using problems where the true UIR is known. This can be done with mathematical test problems degraded with pseudorandom noise.

The application of deconvolution analysis to shunt quantification is unusual in that multimodal input and UIR functions occur with some frequency. Many of the deconvolution algorithms previously used for the characterization of vascular beds have been designed and verified for use with simple unimodal UIR functions (*9–15*). Simulation results on some more general deconvolution algorithms have suggested that they are rather sensitive to random data errors (*6*). Our experience with several of the algorithms previously used for shunt quantification has suggested that sensitivity to noise is a significant problem and may account for some of the oscillatory UIR computed from studies done with fragmented injections (*4*). It is thus desirable to evaluate a deconvolution algorithm capable of accurately handling the range of functions found in shunt quantification. Development of such an algorithm may extend the range of clinical studies that are correctable by deconvolution.

METHODS

We investigated the noise sensitivity of deconvolution algorithms using mathematical test problems. Known input and UIR curves were convolved to obtain a known output curve. The input and output curves were degraded with pseudorandom noise. An estimate of the UIR was obtained by deconvolution of the degraded input and output curves. Reconvolution error was assessed by comparing the degraded output with the convolution of the degraded input and the UIR estimate. UIR error was assessed by comparing the UIR estimate with the known UIR.

General descriptions of the algorithms tested are given below. More detailed information on their implementation is given in the Appendix.

Smooth and non-negative algorithm. This algorithm constrained the UIR to be non-negative and smooth in the sense of having a small sum of squared second or fourth differences. The non-negativity constraint expresses the physically evident fact that the UIR must not be negative. Second and fourth differences are discrete approximations to the second and fourth derivatives respectively. The differences of a function increase with an increase in the rate of change of that function. The sum of squared differences is thus inversely related to the smoothness of a function. Therefore, constraining the UIR to have a small sum of squared differences has the effect of constraining the UIR to be smooth. The use of non-negativity (*6*) and smoothness (*7,8*) constraints in deconvolution has been described in the literature.

Low-pass filter algorithm. The discrete Fourier transform was used to express the exact solution of the convolution equation as the sum of scaled sine and cosine waves of various frequencies. The algorithm constrained the UIR to be smooth in the sense of being primarily composed of low-frequency sinusoidal components. A low-pass filter was used to remove components of frequency greater than a cutoff frequency, ω_c. The filter multiplied the amplitude of the sinusoidal components with frequency $\ll\omega_c$ by a factor close to 1, and the components with frequency $\gg\omega_c$ by a factor close to 0. This has the effect of removing components of frequency greater than ω_c. The UIR was reconstructed by summing the filtered sinusoidal components.

Cubic spline algorithm. A cubic spline is a function composed of a series of cubic polynomial segments with continuous first and second derivatives. Cubic splines are thus a family of relatively smooth functions. The algorithm constrained the UIR to be the cubic spline that minimized the reconvolution error in the least-squares sense.

Lagged normal algorithm. The UIR encountered in shunt quantitation may be decomposed into several components resulting from transit of tracer through the different pathways of the cardiovascular system. A lagged normal curve is a simple unimodal curve similar in shape to the gamma variate function that has been used extensively as a model for the UIR of simple vascular beds. The lagged normal algorithm constrained the UIR to be expressable as the non-negative sum of a set of scaled lagged normal curves. This has the effect of constraining the UIR to be composed of components that might be expected from simple vascular beds. The contribution of each curve was chosen to minimize the reconvolution error in the least-squares sense. The algorithm is a modification of one used in the deconvolution of dye-dilution curves (*16*).

Simulation studies were carried out on a test problem with a unimodal input and UIR proposed by Gamel et al. (*6*) and subsequently studied by Caprihan and Neto (*9*). Since we were interested in deconvolution problems

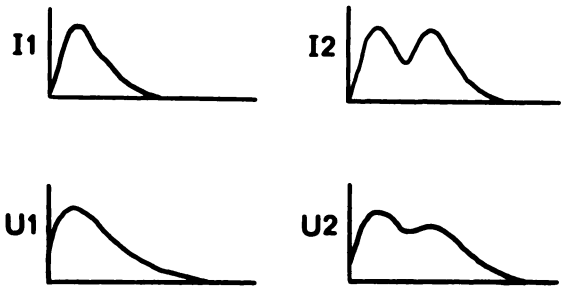

FIG. 1. Curves used in simulation experiments. On top are input functions I1 and I2. At bottom are unit impulse response (UIR) functions U1 and U2.

involving more general functions, we also investigated bimodal input and UIR sequences. The curves tested are shown in Fig. 1. Details of the test problems are in the Appendix. Noise levels of R = 0.01 and R = 0.10 (i.e., 1% and 10%) were investigated.

Means and standard deviations of the UIR- and reconvolution (RC) errors were calculated for each problem using the Euclidean norm expressed as a percentage, as described in Caprihan and Neto (*9*). This differs slightly from the absolute value norm used by Gamel et al. (*6*). The formulae used to compute the error norms are in the Appendix.

RESULTS

Results on the test problems are shown in Table 1. The algorithms tended to perform relatively well at noise level R = 0.01, and less well with R = 0.1. UIR error tended to be higher in test problems using the bimodal input function rather than the unimodal. The smooth and non-negative algorithm and cubic spline algorithm were noteworthy in that performance on the bimodal UIR was much worse than on the unimodal UIR, particularly with noise at R = 0.01. In general, the lagged normal program appeared to perform the best in the sense of having the smallest maximum UIR error over the range of problems tested (see Table 1).

DISCUSSION

Practical application of deconvolution requires the incorporation of additional information describing what constitutes an acceptable UIR into the deconvolution process. This information may be provided by the physical characteristics of the system being studied. For example, in radionuclide angiocardiography the true UIR must be non-negative. Additional information may be incorporated into the deconvolution process in several different ways. The UIR may be constrained to be a member of a specific class of functions, for example, to be non-negative or expressable as the sum of lagged normal curves. Probabilistic information concerning the UIR may be weighted with the data into a statistical estimate of the UIR. For example, smoothness information may be weighted into a least-squares formulation with the data. Additional information may also be expressed as a rule, such as low-pass filtering or smoothing, for obtaining a UIR estimate from an exact solution of the convolution equation.

An ideal deconvolution algorithm would exclude all physically unreasonable solutions while allowing all solutions that are physically possible. This implies that accurate results can be obtained by making all possible use of as much information about the true solution as possible. Use of a non-negativity constraint is advantageous in that it excludes impossible solutions while not making assumptions that need to be tested. Additional information, obtained from characterization of the range of UIR seen in practice, may also be incorporated into the deconvolution process. Use of such information, provided it is correct, allows more accurate UIR estimates.

The most successful program used by Gamel et al. (*6*) on the unimodal input and UIR test problem had a UIR error of more than 11% at the R = 0.01 noise level. Caprihan and Neto (*9*), using more sophisticated modeling techniques, obtained errors of 5 and 12% with noise at R = 0.01 and R = 0.1 respectively. Using the lagged normal algorithm, we were able to reduce these errors to slightly over 2 and 5% respectively.

The algorithms tested in this report have one or more variable parameters which were adjusted to give low UIR errors on the range of problems tested at a particular noise level. Optimum settings for these parameters depend on the signal and noise characteristics encountered in a particular application. These parameters may be thought of as expressing the strength of a preference for a well-behaved solution, as opposed to an exact solution, of the convolution equation. Different settings for them were used at the R = 0.01 and R = 0.1 noise levels, since data degraded with high noise levels require a stronger preference for a well-behaved solution in order to achieve optimal results. The range of UIR encountered in practice might vary more widely than the range of test problems described in this report; in particular the time scale of events may vary several-fold. This may cause greater difficulty in expressing the necessary additional information, and hence a loss of accuracy. Robustness of an algorithm with regard to a large range of UIR is clearly desirable. Results on a deconvolution algorithm similar to the lagged normal algorithm described in this report suggest that the lagged normal algorithm has this property (*16*).

The problem of deconvolution has been examined in the context of quantification of left-to-right shunts from radionuclide angiocardiographic data. Numerical problems that reasonably approximate this real problem were examined to determine which deconvolution methods give the most accurate results. An algorithm that constrained the computed UIR to be expressible as

TABLE 1. PERFORMANCE OF DECONVOLUTION ALGORITHMS ON ANALYTICAL TEST DATA

Noise level	Input curve	UIR curve	Smooth and non-negative algorithm (S = S2)		Smooth and non-negative algorithm (S = S4)		Low-pass filter algorithm (B = 2)		Low-pass filter algorithm (B = 4)		Cubic spline algorithm		Lagged normal algorithm	
			UIR error	RC error	UIR error	RC error	UIR error	RC error	UIR error	RC error	UIR error	RC error	UIR error	RC error
0.01	I1	U1	2.78	0.52	0.97	0.18	13.37	7.25	4.27	1.63	1.25	0.56	2.05	0.54
			±0.57	0.04	0.54	0.06	2.12	0.02	0.13	0.02	0.21	0.04	0.35	0.05
0.01	I1	U2	3.23	0.51	1.95	0.56	11.64	5.19	4.04	1.40	3.90	0.65	2.01	0.52
			±0.54	0.04	0.12	0.03	1.91	0.06	0.23	0.02	0.32	0.05	0.41	0.04
0.01	I2	U1	4.34	0.49	1.99	0.53	14.50	6.02	5.31	1.38	1.90	0.55	2.36	0.54
			±0.86	0.04	0.64	0.05	1.88	0.09	0.40	0.04	0.56	0.05	0.54	0.04
0.01	I2	U2	4.81	0.50	2.57	0.53	14.56	4.49	5.71	1.14	4.33	0.62	2.20	0.56
			±1.45	0.04	1.04	0.04	2.05	0.10	0.81	0.03	0.34	0.05	0.54	0.04
0.10	I1	U1	3.15	5.20	5.18	5.34	21.22	15.06	9.46	6.67	5.86	5.40	5.08	5.41
			±1.45	0.63	2.03	0.48	3.54	0.32	0.91	0.32	1.55	0.53	1.39	0.32
0.10	I1	U2	7.90	5.67	7.82	5.57	17.15	9.98	12.40	6.10	12.89	5.68	6.40	5.47
			±2.13	0.43	2.53	0.26	1.97	0.09	1.17	0.40	5.22	0.47	1.39	0.36
0.10	I2	U1	9.83	5.36	13.05	10.98	21.75	12.63	11.37	7.20	11.38	5.73	7.43	5.39
			±5.36	0.51	10.98	1.25	1.97	0.38	0.80	0.26	6.22	0.26	2.39	0.25
0.10	I2	U2	11.11	5.18	19.26	5.82	19.79	9.98	12.40	6.10	18.36	5.43	7.01	5.64
			±2.60	0.31	15.76	1.33	2.15	0.28	1.53	0.27	5.27	0.50	1.64	0.38

Unit impulse response (UIR) and reconvolution (RC) errors are expressed as mean ± standard deviation of 10 trials.

the non-negative sum of a set of lagged normal curves was found to give the best results. It is suggested that this method be applied to determine whether it improves the clinical evaluation of patients with left-to-right shunts.

ACKNOWLEDGMENT

This work was supported in part by a grant from the Fannie Ripple Foundation, Department of Energy contract EY-76-S-4115. National Institute of Health grant #2-P50-6M-18674-07 and American Heart Association, Greater Boston, MA Division grant #13-523-801. J. Anthony Parker is the recipient of Research Career Development Award 5 K04 HL00465 from the National Heart, Lung, and Blood Institute.

The authors thank Ms. Laurie Pugsley for her assistance in the preparation of this manuscript.

APPENDIX

The relationship of the input, UIR, and output of a discrete, causal, linear, time-invariant system is described by the convolution equation:

$$O_t[i] = \sum_{j=1}^{i} I_t[i-j+1]\, U_t[j] \quad (i = 1,N) \tag{1}$$

$I_t[i]$, $U_t[i]$, and $O_t[i]$ $(i = 1,N)$ are discrete input, UIR, and output sequences in time respectively. Alternatively Eq. (1) can be expressed by the matrix equation:

$$O_t = I_t\, U_t \tag{2}$$

Letting T denote transpose, O_t is the column vector $[O_t[1], O_t[2], \ldots, O_t[N]]^T$, U_t is the column vector $[U_t[1], U_t[2], \ldots, U_t[N]]^T$, and I_t is the lower triangular N × N matrix:

$$I_t[j,k] = \begin{cases} I_t[j-k+1] & j \geq k \\ 0 & j < k \end{cases} \tag{3}$$

We wished to obtain an estimate of U_t, which we will denote as U from noise-degraded measurements of I_t and O_t, which we will denote as I and O respectively.

DESCRIPTION OF THE TEST PROBLEMS

The input sequences used were given by:

$$I1_t[i] = (i\Delta t)^2\, e^{-A(i\Delta t)} \tag{4}$$

and

$$I2_t[i] = \begin{cases} I1_t[i] & (i = 20,N) \\ I1_t[i] + 0.83\, I1_t[i-20] & (i = 21,N) \end{cases} \tag{5}$$

The UIR sequences used were given by:

$$U1_t[i] = (i\Delta t)\, e^{-(i\Delta t)} \tag{6}$$

and

$$U2_t[i] = \begin{cases} U1_t[i] & (i = 1,20) \\ U1_t[i] + 0.7\, U1_t[i-20] & (i = 21,N) \end{cases} \tag{7}$$

Values of A = 2 and $\Delta t = 0.1$ were used. $O_t[i]$ $(i = 1,N)$ was given by direct discrete convolution of the sequences $I_t[i]$ and $U_t[i]$ according to Eq. (1). The observation, I[i] and O[i] $(i = 1,N)$, were obtained by the equations:

$$I[i] = I_t[i]\,(1 + r) \tag{8}$$

and

$$O[i] = O_t[i]\,(1 + r) \tag{9}$$

r was a pseudorandom number uniformly distributed between −R and R. R values of 0.01 and 0.1 were investigated. The simulation experiments were done using input and UIR sequences of 75 points, except in the experiments using the low-pass filter algorithm, which were done using sequences of 128 data points. Longer sequences were used for the low-pass algorithm so that the sequences used were almost equal to zero at their ends. This is important when one is filtering with Fourier transforms, to avoid artifacts due to edge effects (*17*). Ten trials were run for each set of conditions tested. The error norms used were defined as:

$$\text{UIR error} = 100\left\{\sum_{i=1}^{N}(U[i] - U_t[i])^2\right\}^{1/2} \Big/ \left(\sum_{i=1}^{N} U_t[i]^2\right)^{1/2} \tag{10}$$

and

$$\text{RC error} = 100\left\{\sum_{i=1}^{N}(O[i] - I{*}U[i])^2\right\}^{1/2} \Big/ \left(\sum_{i=1}^{N} O[i]^2\right)^{1/2} \tag{11}$$

where * represents the convolution operator.

IMPLEMENTATION OF DECONVOLUTION ALGORITHMS

Smooth and non-negative algorithm. The sum of second or fourth differences of a vector U is given by the product U^TS^TSU where S represents either a second or fourth difference operator. The second and fourth difference operators, denoted as S2 and S4 respectively, were given explicitly by:

$$S2[j,k] = \begin{cases} 1 & (j-k+1 = -1,1) \\ -2 & (j-k+1 = 0) \\ \varnothing & \text{(otherwise)} \end{cases} \tag{12}$$

and

$$S4[j,k] = \begin{cases} 1 & (j-k+1 = -2,2) \\ -4 & (j-k+1 = -1,1) \\ 6 & (j-k+1 = 0) \\ \varnothing & \text{(otherwise)} \end{cases} \tag{13}$$

The operators were not applied to the edges of U. The information $SU = \varnothing$ was incorporated with weight γ into a least-squares formation with the data. Increasing γ has the effect of decreasing the magnitude of U^TS^TSU acceptable in the solution. The UIR was estimated by solving the least-squares problem:

$$\begin{bmatrix} O \\ 0 \end{bmatrix} \cong \begin{bmatrix} I & 0 \\ 0 & \gamma S \end{bmatrix} U \tag{14}$$

for U, subject to the constraint $U \geq 0$. The non-negative least-squares problem expressed by Eq. (14) was solved using the algorithm of Lawson and Hanson (*18*). In the simulation experiments using the second difference operator, S = S2, the parameter γ was set equal to 2 and 20 for noise levels R = 0.01 and R = 0.1 respectively. In the experiments using the fourth difference operator, S = S4, γ was set equal to 100 and 250 for R = 0.01 and R = 0.1 respectively.

Low-pass filter algorithm: The discrete Fourier transform expresses a discrete curve of finite duration as a finite sum of scaled complex exponentials (*17,19*). If the time scale of the observations is properly extended with zeros, it can be shown that the Fourier

coefficients of the exact solution to the convolution equation, UE, are obtained by:

$$UE[\omega] = O[\omega]/I[\omega] \quad (\omega = -\pi\{(N-1)/N\},\pi) \qquad (15)$$

$UE[\omega]$, $O[\omega]$ and $I[\omega]$ are the Fourier coefficients of UE[i], O[i], and I[i] respectively. The Fourier coefficients of U[i] were then obtained from the formula:

$$U[\omega] = A[\omega]\, UE[\omega] \qquad (16)$$

where

$$A[\omega] = 1/\{1 + (\omega/\omega_c)^B\} \quad (\omega = -\pi\{(N-1)/N\},\pi) \qquad (17)$$

This formula describes a low-pass, zero-phase filter known as a Butterworth filter. The parameter ω_c controls the cutoff frequency, and the parameter B controls the steepness of the cutoff at that frequency. Simulation was performed with the parameter B taking on values of 2 and 4. In the experiments using B = 2, the parameter ω_c was set equal to 10 and 6 for noise levels R = 0.01 and R = 0.1 respectively. In the experiments using B = 4, ω_c was set equal to 16 and 10 for R = 0.01 and R = 0.1 respectively.

Cubic spline algorithm. Given an interval divided into a number of subintervals, a cubic spline is a function with continuous first and second derivatives, which can be expressed as a cubic polynomial over each subinterval. The endpoints of the subintervals are known as break points. A cubic spline over NB break points can be expressed as a linear combination of NB + 2 linearly independent basis functions (*18*). Thus, the problem of fitting a cubic spline over NB break points to an N-point curve, H, by least squares takes the form:

$$AC = H \qquad (18)$$

A is a N × NB + 2 matrix of the basis functions, and C is a NB + 2 vector of the amplitudes of the basis functions in the least-squares fit (*18*).

The cubic spline algorithm constrained the computed UIR to a cubic spline over NB evenly spaced break points. It was implemented by solving the least-squares problem:

$$IAC = O \qquad (19)$$

for C. The estimated UIR is given by AC, the cubic spline that minimized the sum of the square reconvolution errors. The number of break points, NB, used in the simulation experiments was 6 and 5 for R = 0.01 and R = 0.1 respectively.

Lagged normal algorithm. The lagged normal curve may be described as the convolution of a normal density curve with a first-order exponential decay curve (*10*). It may be characterized by three parameters, the mean time T_j, the standard deviation about the mean time S_j, and the skewness. The UIR was constrained to be expressable as the non-negative sum of a set of scaled lagged normal curves. The contribution of each lagged normal curve to the UIR was chosen to minimize the sum of the squared reconvolution errors. Twenty lagged normal curves of skewness 1, with T_j geometrically distributed between 5 and 60, were used in the simulation. The S_j values were given by:

$$S_j = S_0 + K\, T_j \qquad (20)$$

An S_0 value of 5 was used in the simulation experiments. K values of 0.2 and 0.3 were used with R = 0.01 and R = 0.1 respectively. The algorithm was implemented using a non-negative least-squares algorithm (*16*).

COMPUTER IMPLEMENTATION

The input and output curves were scaled to one before the start of the computation, and the UIR rescaled appropriately at the end. The programs were written in FORTRAN under the RT-11 operating system and were implemented on a laboratory computer using double-precision (54-bit mantissa, 8-bit exponent) arithmatic.

REFERENCES

1. MALTZ DL, TREVES S: Quantitative radionuclide angiocardiography. Determination of Qp:Qs in children. *Circulation* 47:1049-1056, 1973
2. ASKENAZI J, AHNBERG DS, KORNGOLD E, et al: Quantitative radionuclide angiocardiography: Detection and quantitation of left to right shunts. *Am J Cardiol* 37:382-387, 1976
3. ALDERSON PO, DOUGLASS KH, MENDENHALL KG, et al: Deconvolution analysis in radionuclide quantitation of left-to-right shunts. *J Nucl Med* 20:502-506, 1979
4. HAM HR, DOBBELEIR A, VIART R, et al: Radionuclide quantitation of left-to-right cardiac shunts using deconvolution analysis. *J Nucl Med* 22:688-692, 1981
5. BASSINGTHWAIGHTE JB: Circulatory transport and the convolution integral. *Mayo Clin Proc* 42:137-154, 1967
6. GAMEL J, ROUSSEAU WF, KATHOLI CR, et al: Pitfalls in digital computation of the impulse response of vascular beds from indicator-dilution curves. *Circ Res* 32:516-523, 1973
7. PHILLIPS DL: A technique for the numerical solution of certain integral equations of the first kind. *J Assoc Comput Mach* 9:84-97, 1971
8. HUNT BR: Biased estimation for non-parametric identification of linear systems. *Math Biosci* 10:215-237, 1971
9. CAPRIHAN A, NETO AG: Optimum modeling of vascular beds using indicator-dilution measurements. *IEEE Trans Biomed Eng BME* 24:219-226, 1977
10. BASSINGTHWAIGHTE JB, ACKERMAN FH, WOOD EH: Applications of the lagged normal density curve as a model for arterial dilution curves. *Circ Res* 18:398-415, 1966
11. BASSINGTHWAIGHTE JB: Plasma indicator dispersion in arteries of the human leg. *Circ Res* 19:332-346, 1966
12. BASSINGTHWAIGHTE JB, ACKERMAN FH: Mathematical linearity of circulatory transport. *J Appl Physiol* 22:879-888, 1967
13. KNOPP TJ, BASSINGTHWAIGHTE JB: Effect of flow on transpulmonary circulatory transport functions. *J Appl Physiol* 27:36-43, 1969
14. ROSENKRANTZ JG, MALONEY JC: Pseudorandom noise and cross-correlation in indicator-dilution systems. *J Surg Res* 21:105-111, 1976
15. POLLASTRI A, PISTOLESI M, GIUNTINI K: A method for computing frequency functions from input-output vascular dilution curves. *J Nucl Med Allied Sci* 21:165-172, 1977
16. KNOPP TJ, DOBBS WA, GREENLEAF JF, BASSINGTHWAIGHTE JB: Transcoronary intravascur transport functions obtained via a stable deconvolution technique. *Ann Biomed Eng* 4:44-59, 1976
17. OPPENHEIN AV, SCHAFER RW: Digital signal processing. Prentice-Hall Inc., Englewood Cliff, NJ, 1975
18. LAWSON CL, HANSON RJ: Solving least squares problems. Prentice-Hall, Inc., Englewood Cliffs, NJ, 1974
19. NIEMI AJ: On discrete deconvolution. *Med Biol Eng* 15: 582-584, 1976